Structure and stability of crystals under anisotropic stress

P M Marcus and F Jona

Department of Materials Science and Engineering, State University of New York, Stony Brook, NY 11794-2275, USA

Abstract
A first-principles calculation procedure is given for determining the structure, elastic response and stability of a crystal in equilibrium under anisotropic stress. Under a strain the change in internal energy plus the work done by the crystal is shown to be a minimum with respect to structural changes, and to be expandable in powers of the Eulerian strains. The coefficients of second-order terms in the expansion are shown to be effective elastic constants for the equilibrium crystal which determine stability. Application to body-centered tetragonal (bct) Al leads to evaluation of lattice parameters as functions of lateral and longitudinal stresses. Two stable bct phases at a given longitudinal stress are found, one with the lateral stress mainly larger and one with lateral stress smaller than the longitudinal stress. The stability of the structure in each of these bct phases is established by showing that all the eigenvalues of the effective elastic constant matrix are positive.

1. Introduction

The equilibrium properties of crystals under stress show substantial change from these properties at zero stress. Application of hydrostatic pressure has led to large changes in three equilibrium properties: structure, elastic response and stability, including discontinuous changes to new phases. First-principles band-structure programs have calculated these three properties as functions of hydrostatic pressure with good accuracy. However the effects of anisotropic stress on these properties would be a vast expansion of basic knowledge of crystals that has not been made. Complications have arisen in the analysis of properties under anisotropic stress such as the lack of an equilibrium Gibbs free energy, the fact that the elastic constants for stress–strain relations are different from the elastic constants in the elastic equations of motion, and the fact that both kinds of elastic constants do not have the full Voigt symmetry in their four-index components [1, 2].

Here we treat the effects of anisotropic stress in a crystal *in equilibrium* under that stress in a way that avoids all the complications noted above. We expand both δE, the change in internal

energy of the crystal, and δW, the sum of the work done by the stress in the crystal at each face on a reservoir that balances the stress at that face, in a power series in the six components of Eulerian strains. The expansions in these strains, which can describe the nonrotational part of any homogeneous deformation, are carried to second order in the strains. The two-index coefficients of the second-order terms in $\delta E + \delta W$ are shown to act as effective elastic constants which determine elastic response and stability of the equilibrium state, since $\delta E + \delta W$ is shown to have a minimum property like $\delta G = \delta E + p\delta V$ in the hydrostatic case. A first-principles calculation is carried out on body-centered tetragonal (bct) Al which shows how the structure, elastic response and stability vary as the two stress components (σ_1 laterally and σ_3 longitudinally) on equilibrium bct Al vary. An interesting new feature is that as the magnitude of σ_1 drops below the magnitude of σ_3 a range of instability and discontinuous structural changes occurs.

Section 2 gives the general formulation which justifies the expansion in strain components and leads to the interpretation of the second-order coefficients as effective elastic constants. Section 3 describes the first-principles calculation procedures which find the stresses in a given structure, the effective elastic constants and the stability of the structure. Section 4 describes the calculations' results that show how the structure and stability vary as functions of σ_1 and σ_3. In section 5 we discuss the significance of unstable ranges of anisotropic stress for experiment, the validity of the two-index elastic constants and their relation to the standard four-index elastic constants.

2. General formulation

A homogeneous Bravais crystal of specified structure, i.e., of given values of the lattice vectors **a**, **b**, **c** that generate the lattice, has values of volume V per atom, internal energy E per atom and stresses σ_i, $i = 1$–6, that can be calculated from first principles with good accuracy. Any homogeneous deformation of the given structure can be described by a set of Eulerian strains ϵ_i, $i = 1$–6, ($\{\epsilon_i\}$) after rigid rotations have been taken out [3].

The lattice vectors of the strained structure $\mathbf{a}'$, $\mathbf{b}'$, $\mathbf{c}'$ are functions of the $\{\epsilon_i\}$ through matrix equations [3]

$$
\underline{\boldsymbol{\epsilon}} = \begin{pmatrix} \epsilon_1 & \epsilon_6/2 & \epsilon_5/2 \\ \epsilon_6/2 & \epsilon_2 & \epsilon_4/2 \\ \epsilon_5/2 & \epsilon_4/2 & \epsilon_3 \end{pmatrix}, \qquad \underline{\mathbf{R}} = \begin{pmatrix} a_1 & b_1 & c_1 \\ a_2 & b_2 & c_2 \\ a_3 & b_3 & c_3 \end{pmatrix}, \qquad \underline{\mathbf{R}}' = \begin{pmatrix} a_1' & b_1' & c_1' \\ a_2' & b_2' & c_2' \\ a_3' & b_3' & c_3' \end{pmatrix},
$$
$$
\underline{\mathbf{R}}' = (\underline{\mathbf{I}} + \underline{\boldsymbol{\epsilon}})\underline{\mathbf{R}}, \tag{1}
$$

where $\underline{\boldsymbol{\epsilon}}$ is the strain matrix, $\underline{\mathbf{I}}$ is the identity matrix, and the $a_i, b_i, c_i, a_i', b_i', c_i'$, $i = 1, 2, 3$ are components in orthogonal axes.

Since E can be calculated for any $\underline{\mathbf{R}}'$, δE is a function of the $\{\epsilon_i\}$ and we can expand δE around the specified structure for small values of $\{\epsilon_i\}$ in a power series; to second order the series is

$$
\frac{\delta E}{V_0} \equiv \frac{E - E_0}{V_0} = \sum_{i=1}^{6} \overline{c_i}\epsilon_i + \frac{1}{2}\sum_{i,j=1}^{6} \overline{c_{ij}}\epsilon_i\epsilon_j, \tag{2}
$$

where V_0, E_0 refer to the specified original structure $\underline{\mathbf{R}}$ and E to the strained structure $\underline{\mathbf{R}}'$.

The stresses σ_i in the crystal *at equilibrium* are defined as

$$
\sigma_i = \frac{1}{V_0}\left(\frac{\partial E}{\partial \epsilon_i}\right)_0 = \overline{c_i}, \tag{3}
$$

where $\epsilon_j = 0$, $j \neq i$. If the stresses $\overline{c_i}$ in the original state are balanced by equal and opposite stresses applied to the six separate faces of the crystal by external reservoirs, the original

crystal is in a constrained-equilibrium state of anisotropic stress. This state is analogous to the constrained-equilibrium states under hydrostatic pressure applied by an external reservoir on all faces to balance an internal pressure.

In the state of constrained equilibrium the crystal has well-defined elastic responses and a stability dependent on that response that will be determined here. These features in the hydrostatic case are easily found from a Gibbs free energy $G = E + pV$ (at $T = 0$). For the anisotropic case we need a replacement for G.

Actually it will be adequate to find a replacement for δG around the equilibrium state, which will have an expansion in $\{\epsilon_i\}$ to second order that will give the elastic response and stability for small strains. We need the analogue of the theorem that G is a minimum in equilibrium at constant pressure, since in the hydrostatic case elastic response comes from the curvature of $\delta G(\{\epsilon_i\})$ and stability from the positive definiteness of δG for all $\{\epsilon_i\}$. In the present case we apply the thermodynamic theorem that the internal energy of a closed system is a minimum at equilibrium. If the closed system is the crystal plus the reservoirs that apply the external stresses, then the theorem states that $\delta E + \delta W > 0$ for all $\{\epsilon_i\}$, where δE is the change in E of the crystal and δW is the work done by the crystal on the reservoirs (which increases the internal energy of the reservoirs). For hydrostatic pressure p we have $\delta W = p\delta V$ and the stability condition is $\delta E + p\delta V = \delta G > 0$, but for anisotropic stress δW will be broken up into separate contributions from the individual stresses on each face of the unit cell.

In the hydrostatic case at equilibrium

$$\frac{\delta G}{V_0} = \frac{1}{2} \sum_{i,j=1}^{6} c_{ij} \epsilon_i \epsilon_j, \tag{4}$$

where the c_{ij} are the elastic constants. Similarly in the anisotropic-stress case at equilibrium we have

$$\frac{\delta E + \delta W}{V_0} = \frac{1}{2} \sum_{i,j=1}^{6} \overline{c_{ij}} \epsilon_i \epsilon_j + \frac{1}{2} \sum_{i,j=1}^{6} \tilde{c_{ij}} \epsilon_i \epsilon_j \equiv \frac{1}{2} \sum_{i,j=1}^{6} c_{ij} \epsilon_i \epsilon_j, \tag{5}$$

where the $\tilde{c_{ij}}$ come from the terms in δW second order in the $\{\epsilon_i\}$, and

$$c_{ij} \equiv \overline{c_{ij}} + \tilde{c_{ij}}. \tag{6}$$

The first-order terms in $\{\epsilon_i\}$ in δE and δW cancel, just as in the hydrostatic case.

We now evaluate $\overline{c_{ij}}$ and $\tilde{c_{ij}}$ in the specific case of body-centered tetragonal (bct) Al from first principles. There are two structural parameters a_{bct} and c_{bct}, and two stress components σ_1 on the lateral faces and σ_3 on the longitudinal faces in orthogonal axes x_1, x_2, x_3 with x_3 along the c_{bct} axis, x_1 and x_2 along the sides of the square tetragonal face. We will find as functions of σ_1 and σ_3 the parameters a_{bct}, c_{bct}, $\overline{c_{ij}}$, $\tilde{c_{ij}}$, c_{ij}. Instability will be found from a negative eigenvalue of the $6 \times 6 \{c_{ij}\}$ matrix, which indicates that $\frac{1}{2} \sum_{i,j=1}^{6} c_{ij} \epsilon_i \epsilon_j$ is not positive definite.

The development here is similar to that of Wang *et al* [4]. In [4] a Gibbs driving force is defined as the sum of an energy (the Helmholtz free energy) change and a work term along a deformation path. This driving force is expanded in strain components to give elastic constants as coefficients in the expansion. The positive definiteness of a quadratic form in the strains with these elastic coefficients is used as a criterion of stability. Our development uses the simpler Eulerian strains where Wang *et al* use Lagrangian strains, but we are careful to expand to second order in the Eulerian strains. We also simplify by using the simpler Voigt indices on strains, stresses and second-order expansion coefficients. We use the procedures established in previous work to find quantitative values of the structure, elasticity and stability of tetragonal equilibrium states of Al under anisotropic tetragonal stresses where (5) replaces (4); the stresses from (3) can range over the entire σ_1–σ_3 plane as a and c change.

3. Calculation procedures

3.1. Background

The starting point is the epitaxial Bain path (EBP) of bct Al, initially assumed to be at zero applied pressure, $p = 0$. Recall that a Bain path is a path in the tetragonal plane (defined by the tetragonal lattice parameters $a = a_{bct}$ and $c = c_{bct}$) that goes through various bct energy minima, and the EBP is the unique Bain path along which the stress in the c direction vanishes [5]. Accordingly, the EBP is calculated by finding at each value of a the value of c at which the stress along c is

$$\sigma_3 = \frac{1}{V}\left(\frac{\partial E}{\partial \epsilon_3}\right)_{\epsilon_1} = \frac{2}{a^2}\left(\frac{\partial E}{\partial c}\right)_a = 0, \tag{7}$$

where E is the energy, ϵ_3 the strain in the c direction, and the volume $V = a^2 c/2$.

The EBP of bct Al at $p = 0$ is plotted in the form of E versus a in the top panel of figure 1[1]. At the minima of E along the EBP the transverse stresses $\sigma_1 = \sigma_2$ vanish since

$$\sigma_1 = \sigma_2 = \frac{1}{V}\left(\frac{\partial E}{\partial \epsilon_1}\right)_{\epsilon_3} = \frac{2}{ac}\left(\frac{\partial E}{\partial a}\right)_c = 0. \tag{8}$$

The deepest minimum of E is found here to be at $a = a_{bct} = 2.854$ Å, $c = c_{bct} = 4.0524$ Å, in good agreement with the experimental value for face-centered cubic (fcc) Al $a_{fcc} = 4.0496$ Å [9]. At points away from the minima along the EBP σ_3 is still 0 by construction, but the in-plane stress $\sigma_1 = \sigma_2$ is finite and changes in magnitude for different states along the EBP. Hence calculating σ_1 along the EBP satisfies one goal of the present work to determine σ_1 as a function of structure.

If we wish to find equilibrium of a crystal under a finite hydrostatic pressure p, the EBP can be generalized by substituting for the condition (7) the new condition $\sigma_3 = -p$, and by seeking a minimum of the Gibbs free energy per atom at p (at $T = 0$ to cancel the entropy term) *defined* by $G = E + pV$ [5]. We have calculated (see footnote 1) both E and G for bct Al under three different pressures: 600, 1200 and 1840 kbar (10 kbar = 1 GPa); they are plotted in the three lower panels of figure 1. For each p the deepest minimum of G determines the equilibrium structure of Al at that pressure, since at that point the in-plane stress σ_1 is also $-p$, thus establishing hydrostatic conditions. Figure 2 shows the calculated pressure dependence of a_{fcc}, in good agreement with the experimental data of Akahama *et al* above 1800 kbar, as already reported in [10]. For each state along the generalized EBP the in-plane stress σ_1 varies, a variation that we will presently determine.

### 3.2. Calculation of the lateral stress σ_1 for a given σ_3

At each point $(a_1 = a_2, c_1)$ along the E curve on the EBP at p

$$\sigma_3 = \frac{c_1}{V_1}\left(\frac{\partial E}{\partial c_1}\right)_a, \qquad \sigma_1 = \frac{a_1}{V_1}\left(\frac{\partial E}{\partial a_1}\right)_c, \tag{9}$$

[1] The calculations were done with the WIEN2k computer program developed by Blaha and co-workers [6]. This program uses the FPLAPW method for computation of the electronic structure of solids from the Kohn–Sham equations of density functional theory [7, 8]. The calculations in this work were done with the semi-relativistic GGA and with the following parameters: muffin-tin radius of Al $RMT = 1.9$ bohr; criterion for energy convergence 1×10^{-6} Ryd; plane-wave cutoff $RK_{max} = 9$; largest vector in the charge-density Fourier expansion $GMAX = 16$ bohr^{-1}; k-point sampling in the Brillouin zone of 32 000 points (2180 in the irreducible wedge of the Brillouin zone, IBZ) for the EBP computations, and 8000 points (700 in the IBZ) for the $\{c_{ij}\}$ calculations.

4
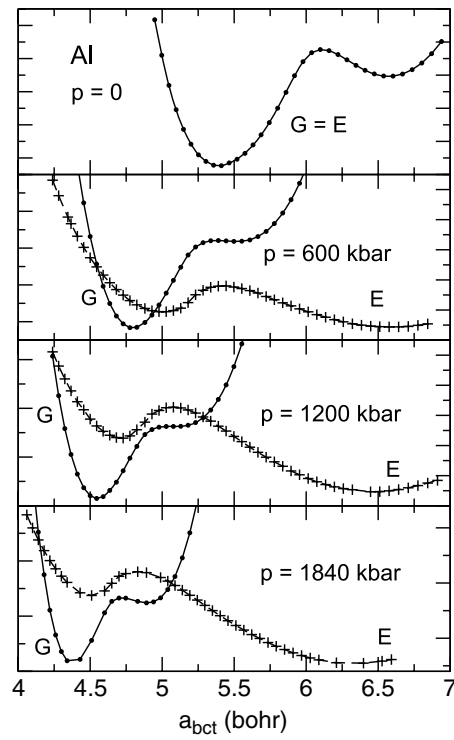
Figure 1. Epitaxial Bain paths (EBPs) for Al at the pressures p indicated. E is the energy, G the Gibbs free energy $G = E + pV$ at $T = 0$ K (V = volume per atom).
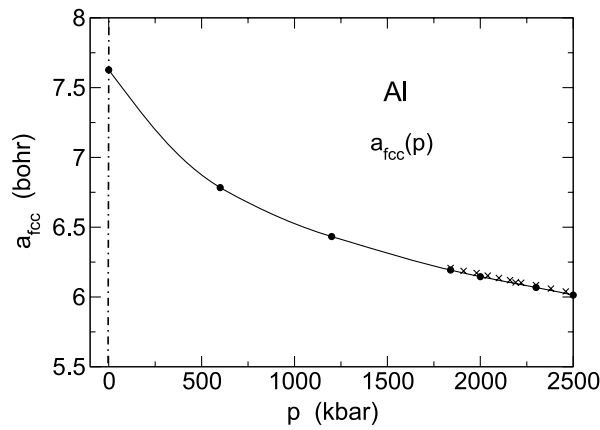
Figure 2. Pressure dependence of the lattice constant a_{fcc} of face-centered cubic Al. Solid circles, calculated values; crosses, experimental values of Akahama *et al* [11].

where $V_1 = c_1 a_1^2/2$. If both a_1 and a_2 are changed to a, then

$$\frac{\partial E}{\partial a} = \frac{\partial E}{\partial a_1}\frac{\partial a_1}{\partial a} + \frac{\partial E}{\partial a_2}\frac{\partial a_2}{\partial a} = 2\frac{\partial E}{\partial a_1}, \tag{10}$$

(since $\partial a_1 / \partial a = \partial a_2 / \partial a = 1$). Replacing $\partial E / \partial a_1$ by σ_1 in (9) we find

$$\sigma_1 = \frac{a}{2V} \left(\frac{\partial E}{\partial a} \right)_c = \sigma_2, \tag{11}$$

where $V = c \, a^2 / 2$.

To find σ_1 we will use the derivative of E along the EBP combined with $(\partial E / \partial c)_a$; we start from the derivative of E with respect to the distance s along the EBP arc length:

$$\frac{dE}{ds} = \left(\frac{\partial E}{\partial a} \right)_c \frac{da}{ds} + \left(\frac{\partial E}{\partial c} \right)_a \frac{dc}{ds}, \tag{12}$$

whence

$$\left(\frac{\partial E}{\partial a} \right)_c = \left[\frac{dE}{ds} - \left(\frac{\partial E}{\partial c} \right)_a \frac{dc}{ds} \right] \bigg/ \frac{da}{ds}. \tag{13}$$

Now from $\sigma_3 = (c/V)(\partial E / \partial c)_a = -p$ we get

$$\left(\frac{\partial E}{\partial c} \right)_a = -\frac{p \, V}{c} \tag{14}$$

hence from (11) and (12)

$$\sigma_1 = \frac{a}{2V} \left[\frac{dE}{ds} - \frac{p \, V}{c} \frac{dc}{ds} \right] \bigg/ \frac{da}{ds}. \tag{15}$$

For the derivatives with respect to s we construct a table with successive values of E, a, c, and s (with s the distance along the EBP from a reference point, e.g. the minimum) and calculate the d/ds derivatives needed in (15). Thus for any pressure p, i.e. for constant $\sigma_3 = -p$, we will find the value of the in-plane stress σ_1 associated with each pair of a and c parameters.

3.3. Stability of structures under anisotropic stress

We now address the question of stability of the structures found above which are in constrained equilibrium under longitudinal stress σ_3 and transverse stress σ_1. The goal is to find the effective elastic constants c_{ij} of those structures and then to examine whether or not the eigenvalues of the $\{c_{ij}\}$ matrix are positive, as discussed in section 2. For each (a, c) state along the EBP we apply the procedure described in the following.

To evaluate the coefficients in (5) we consider the terms δE and δW separately. First we examine the strain terms in δE. For tetragonal structures (2) contains 2 first-order and 6 second-order terms as follows

$$\frac{\delta E}{V} = \overline{c_1}(\epsilon_1 + \epsilon_2) + \overline{c_3}\epsilon_3 + \frac{1}{2}\overline{c_{11}}(\epsilon_1^2 + \epsilon_2^2) + \frac{\overline{c_{33}}}{2}\epsilon_3^2 + \frac{\overline{c_{44}}}{2}(\epsilon_4^2 + \epsilon_5^2)$$
$$+ \frac{\overline{c_{66}}}{2}\epsilon_6^2 + \overline{c_{12}}\epsilon_1\epsilon_2 + \overline{c_{13}}(\epsilon_1\epsilon_3 + \epsilon_2\epsilon_3). \tag{16}$$

We will not consider the shearing constants $\overline{c_{44}}$ and $\overline{c_{66}}$, which are associated with strains shearing tetragonal symmetry.

For each (a, c) state, we calculate the energy E for two strains $\pm\epsilon_1$, $\epsilon_i = 0$, $i \neq 1$ so that

$$\frac{1}{V}\delta E^{(1)} = \overline{c_1}\epsilon_1 + \frac{1}{2}\overline{c_{11}}\epsilon_1^2, \tag{17}$$

$$\frac{1}{V}\delta E^{(2)} = -\overline{c_1}\epsilon_1 + \frac{1}{2}\overline{c_{11}}\epsilon_1^2. \tag{18}$$

Then

$$\frac{1}{V}\delta E^{(1)} - \frac{1}{V}\delta E^{(2)} = 2\overline{c_1}\epsilon_1, \tag{19}$$

$$\frac{1}{V}\delta E^{(1)} + \frac{1}{V}\delta E^{(2)} = \overline{c_{11}}\epsilon_1^2. \tag{20}$$

Thus (19) and (20) evaluate $\overline{c_1}$ ($\equiv \sigma_1$) and $\overline{c_{11}}$, respectively. Similarly the strains $\pm\epsilon_3$, $\epsilon_i = 0$, $i \neq 3$ give $\overline{c_3}$ ($\equiv \sigma_3$) and $\overline{c_{33}}$.

With a strain $\epsilon_1 = \epsilon_2$ ($= e$), $\epsilon_3 = \epsilon_4 = \epsilon_5 = \epsilon_6 = 0$,

$$\frac{1}{V}\delta E^{(3)} = 2\overline{c_1}e + (\overline{c_{11}} + \overline{c_{12}})e^2. \tag{21}$$

Then substitution of $\overline{c_1}$ from (19) and $\overline{c_{11}}$ from (20) in (21) gives $\overline{c_{12}}$. Similarly $\overline{c_{13}}$ is obtained from $\epsilon_1 = \epsilon_3 = e$, $\epsilon_2 = \epsilon_4 = \epsilon_5 = \epsilon_6 = 0$.

Next we want to find the coefficients $\tilde{c}_{ij}$ of the second-order terms in the expansion of δW in Eulerian strains to use in (6) to find the c_{ij}. This calculation for bct structure is most easily carried out with the rectangular two-atom bct cell with lattice vectors $\mathbf{a} = \mathbf{a}_{bct}$, $b = a$ and $\mathbf{c} = \mathbf{c}_{bct}$. Then the two stresses σ_1 and σ_3 are in the direction of orthogonal axes along the sides of the rectangular cell, the faces are perpendicular to these axes and the movement of the faces in the strains used for δE is along these same axes, hence the strains only change the bct structure into an orthorhombic one, but the orientation of faces and their movements remain in the bct directions.

So in the simple case of the rectangular cell, δW is made up of just three terms, one for each face, e.g. for the $\mathbf{b}$–$\mathbf{c}$ face the work is the outward force on the $\mathbf{b}$–$\mathbf{c}$ surface given by $-\sigma_1(\mathbf{b} \times \mathbf{c}) \cdot \hat{\mathbf{x}}_1$ acting through the displacement of $\delta\mathbf{a} \cdot \hat{\mathbf{x}}_1$ where $\delta\mathbf{a} \equiv \mathbf{a}' - \mathbf{a}$ and $\hat{\mathbf{x}}_1$ is the unit vector along $\mathbf{a}$.

Since the $\mathbf{b}$–$\mathbf{c}$ face changes to $\mathbf{b}'$–$\mathbf{c}'$ linearly with the strain we use the average value of the face area to write compactly for δW for the rectangular cell

$$\delta W = -\sigma_1\left(\frac{\mathbf{b} \times \mathbf{c}}{2} + \frac{\mathbf{b}' \times \mathbf{c}'}{2}\right) \cdot \delta\mathbf{a} - \sigma_1\left(\frac{\mathbf{c} \times \mathbf{a}}{2} + \frac{\mathbf{c}' \times \mathbf{a}'}{2}\right) \cdot \delta\mathbf{b}$$
$$- \sigma_3\left(\frac{\mathbf{a} \times \mathbf{b}}{2} + \frac{\mathbf{a}' \times \mathbf{b}'}{2}\right) \cdot \delta\mathbf{c}. \tag{22}$$

Actually we need just the part of δW that is second order in the strains. From (22) this part is

$$\delta W_2 = -\sigma_1\left(\frac{\mathbf{b} \times \delta\mathbf{c} \cdot \delta\mathbf{a}}{2} + \frac{\delta\mathbf{b} \times \mathbf{c} \cdot \delta\mathbf{a}}{2}\right) - \sigma_1\left(\frac{\mathbf{c} \times \delta\mathbf{a} \cdot \delta\mathbf{b}}{2} + \frac{\delta\mathbf{c} \times \mathbf{a} \cdot \delta\mathbf{b}}{2}\right)$$
$$- \sigma_3\left(\frac{\mathbf{a} \times \delta\mathbf{b} \cdot \delta\mathbf{c}}{2} + \frac{\delta\mathbf{a} \times \mathbf{b} \cdot \delta\mathbf{c}}{2}\right). \tag{23}$$

Then $\delta E + \delta W_2/2$ is the value per atom, which can be used directly to find the c_{ij}, just as δE alone was treated in (17)–(21) to find the $\overline{c_{ij}}$.

Note that the volume change per atom $\delta V = V - V_0$ can be expanded in products of δa, δb, δc up to third order, since

$$\delta V \equiv V - V_0 = (\mathbf{a} + \delta\mathbf{a}) \times (\mathbf{b} + \delta\mathbf{b}) \cdot (\mathbf{c} + \delta\mathbf{c}) - \mathbf{a} \times \mathbf{b} \cdot \mathbf{c}. \tag{24}$$
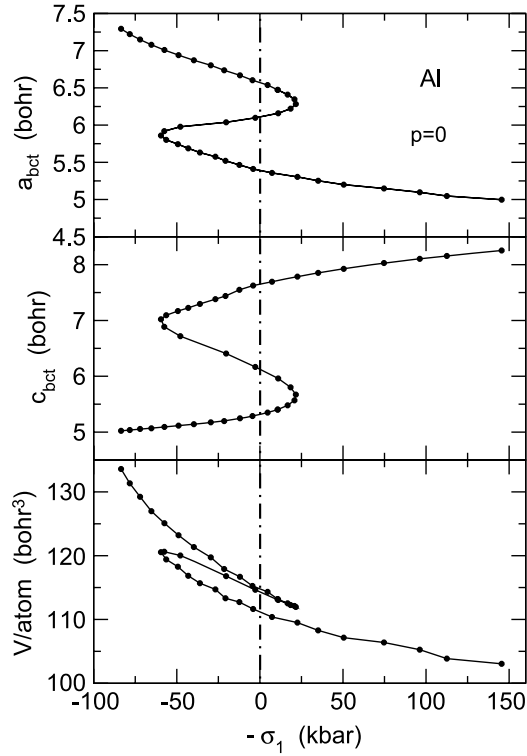
Hence the second-order part per atom is

$$\delta V_2 \equiv (V - V_0)_2 = \frac{\mathbf{a} \times \delta\mathbf{b} \cdot \delta\mathbf{c}}{2} + \frac{\delta\mathbf{a} \times \delta\mathbf{b} \cdot \mathbf{c}}{2} + \frac{\delta\mathbf{a} \times \mathbf{b} \cdot \delta\mathbf{c}}{2}. \tag{25}$$

Then the substitution $\sigma_1 = \sigma_3 = -p$ in (23) gives for $\delta W/2$

$$\frac{\delta W_2}{2} = p\,\delta V_2, \tag{26}$$

which is the correct work term in the hydrostatic case per atom.

Figure 3. Lattice parameters a_{bct}, c_{bct} and volume per atom V of bct Al as functions of $-\sigma_1$ (transverse stress) at $-\sigma_3 = p = 0$.

Note that the six volume-change terms in (23) per rectangular cell combine to give (twice) the three terms of (25) per atom when $\sigma_1 = \sigma_3$. Note also that when the origin remains in one corner of the rectangular cell, all three faces attached to the origin do not change and all the work is done at the three unattached faces which give the three terms in (22).

Applying to δW_2 the same procedure that was used to calculate the $\overline{c_{ij}}$ for δE will produce the $\tilde{c}_{ij}$ that appear in (5). Then (6) will produce the c_{ij}. Finally, calculation of the eigenvalues of the c_{ij} matrix at each (a, c) value will test the stability of the (a, c) state under consideration. A negative eigenvalue means that an eigenfunction exists, i.e. a strain exists, which makes $(1/2) \sum c_{ij} \epsilon_i \epsilon_j$ negative, hence $\delta E + \delta W$ is not at a minimum at that (a, c).

4. Results

Since by convention a negative stress corresponds to a compression, in the following figures we plot various quantities versus $-\sigma_1$ in order to adhere to normal intuition, so that, e.g., $-\sigma_1 = 150$ kbar means 150 kbar compression.

Consider first the case $p = -\sigma_3 = 0$. In figure 3 we plot, in three panels, the results of calculations of a_{bct}, c_{bct} and $V =$ volume/atom versus $-\sigma_1$. For a_{bct} (upper panel) we distinguish three branches: a lower branch which goes from about 150 kbar compression through 0 to about 58 kbar tension; an intermediate branch from 58 kbar tension through 0 to about 22 kbar compression; and an upper branch from 22 kbar compression through 0 to about 90 kbar tension. The state at $-\sigma_1 = 0$ in the lower branch corresponds to the case
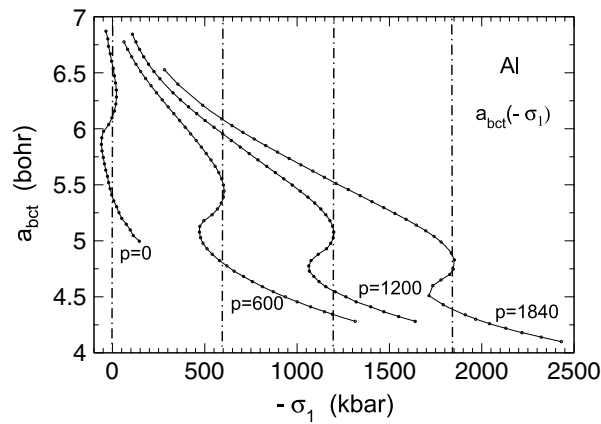
Figure 4. Lattice parameters a_{bct} of bct Al at constant $-\sigma_3 = p = 0, 600, 1200, 1840$ kbar, as indicated, as functions of $-\sigma_1$.
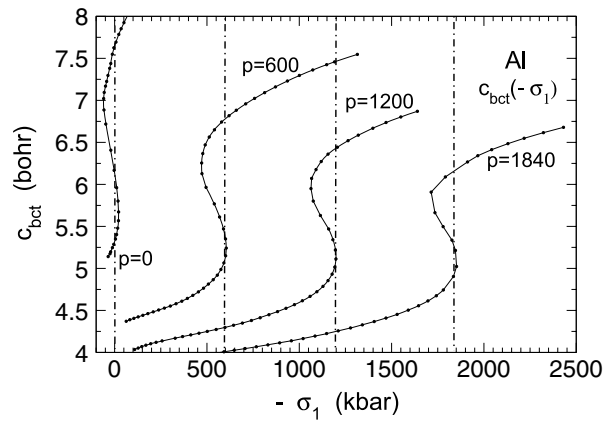

Figure 5. Lattice parameters c_{bct} of bct Al at constant $-\sigma_3 = p = 0, 600, 1200, 1840$ kbar, as indicated, as functions of $-\sigma_1$.

of the crystal in vacuum, the equilibrium state at zero pressure. It is expected that several of the states represented by the full circles in figure 3 will be unstable, which is what we will determine below. Similar considerations apply, *mutatis mutandis*, to $c_{bct}(-\sigma_1)$ (middle panel) and to $V(-\sigma_1)$ (bottom panel).

At finite pressures the dependence of the lattice parameters on $-\sigma_1$ is similar, but the curves shift toward larger compressions, as shown in figures 4 and 5. For the three pressures considered here ($p = -\sigma_3 = 600, 1200$ and 1840 kbar) the (a_{bct}, c_{bct}) states associated with $-\sigma_1 = 600, 1200$ and 1840 kbar, respectively (i.e. for $\sigma_1 = \sigma_3$) on the lower branches are under hydrostatic pressure. All the others are states under anisotropic stress since $\sigma_1 \neq \sigma_3$.

The information provided by these figures is of practical interest for the following reason. In an experiment in which the pressure applied along the c axis has a known value, say, 1200 kbar (e.g. in a diamond-anvil-cell experiment), but hydrostatic conditions may not apply (intentionally or otherwise) the pertinent curves in figures 4 and 5 show which structure will be found depending upon the magnitude of the transverse stress σ_1. The structure will be under anisotropic stress.
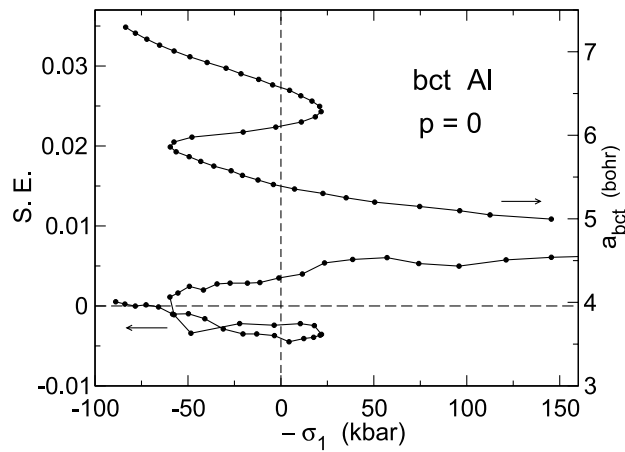
Figure 6. Magnitude of the smallest eigenvalue (SE) of the $\{c_{ij}\}$ matrix (left scale) and of the a_{bct} parameter (right scale) of bct Al versus $-\sigma_1$ at $-\sigma_3 = p = 0$.
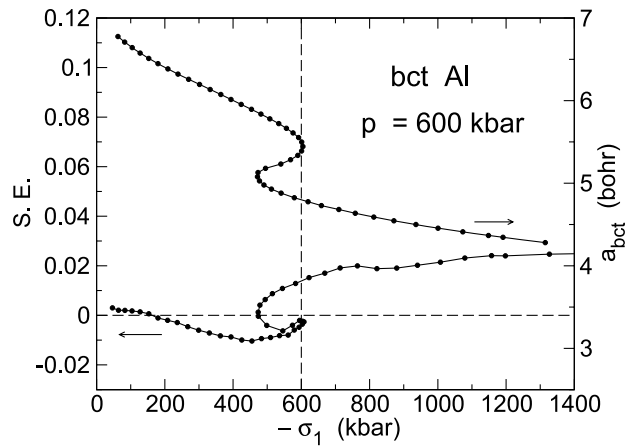
Figure 7. Magnitude of the smallest eigenvalue (SE) of the $\{c_{ij}\}$ matrix (left scale) and of the a_{bct} parameter (right scale) of bct Al versus $-\sigma_1$ at $-\sigma_3 = p = 600$ kbar.

What remains to be established is whether the structure is stable. The procedure described in section 3.3 provides the answer, as summarized in figures 6 and 7 for the cases $p = -\sigma_3 = 0$ and $p = -\sigma_3 = 600$ kbar, respectively. The figures show the values of the smallest eigenvalue of the $\{c_{ij}\}$ matrix for all states along the EBPs of figure 1 for the two values of σ_3 considered here. In figures 6 and 7 we have also redrawn, for convenience, the curves of $a_{bct}(-\sigma_1)$ that appear in figures 4 and 5. We see that all states on the lower branch of the $a_{bct}(-\sigma_1)$ curves are stable, since all eigenvalues of the $\{c_{ij}\}$ matrix are positive, but the states on the intermediate and part of the upper branch are unstable. Interestingly, states with larger a_{bct} values (at the leftmost end of the upper branches considered here) are stable again, so that a hypothetical experiment carried out with decreasing lateral stress at constant longitudinal stress would reveal a discontinuous change in lattice parameters and formation of another phase. We have not done the calculation of eigenvalues of $\{c_{ij}\}$ for the cases of $p = 1200$ and 1840 kbar, but we expect that their behavior will be similar to that shown in figures 6 and 7.

5. Discussion

The problem studied here is a more restricted one than Barron and Klein [1] or Wallace [2] discuss. We study an equilibrium state achieved by finding the anisotropic stresses in a crystal with a given structure and then matching those anisotropic stresses with equal and opposite stresses applied to the faces of the crystal. In [1] and [2] an arbitrary anisotropic stress is imposed on a crystal with a given structure and equilibrium is not sought or mentioned. But by starting with equilibrium we deal with stresses with the symmetry of the given structure and can focus on strains related to that symmetry, e.g., the rectangular axes of bct Al. When the imposed stresses are arbitrary, the crystal is not in equilibrium and will change with time. An equilibrium may be reached with time, but the theory would have to solve for that equilibrium structure. Experiments that are stationary in time will generally measure the equilibrium structures to which our calculations apply as the applied stresses change.

In [1] and [2] the internal energy is expanded in power series in the strains with first-order and second-order terms dependent on the applied stresses. In our formulation we can expand $\delta E + \delta W$ in strains and invoke a minimum principle at equilibrium that makes the first-order terms vanish and allows the second-order terms to function as an elastic response which determines stability in states of anisotropic stress.

The procedure described here and illustrated for bct Al seems generalizable to any symmetry and crystal, i.e. assume structure, find stresses to balance for equilibrium (including relaxation of all atomic positions not fixed by symmetry) and expand $\delta E + \delta W$ around equilibrium in six components of Eulerian strain to find two-index effective elastic constants as coefficients of second-order terms.

The bct case required just three work terms, one for each face, since the faces are perpendicular to the orthogonal axes and the stresses have only components along the axes. For the case of no symmetry each face would need to be projected on three axis planes, and three work terms calculated on each of those planes using the three components of stress on that plane—a total of 27 contributions.

The results for bct Al show variation of structure and stability as σ_3 and σ_1 vary and could cover all values of σ_1 and σ_3. They show that a_{bct} decreases and c_{bct} increases as the lateral compressive stress $(-\sigma_1)$ increases. But a_{bct} and c_{bct} turn out to be multivalued functions of σ_1 in certain ranges, and what might be called a 'turnaround region' exists. Starting from the high-compression behavior (large values of $-\sigma_1$) a_{bct} increases as the lateral compression decreases until $-\sigma_1$ reaches a minimum and the a_{bct} values enter a second branch in which a_{bct} increases as compression increases—a generally unstable situation. But a second turnaround occurs and a_{bct} again increases on a third branch as the compression starts to decrease. This turnaround behavior occurs for both a_{bct} and c_{bct} at all values of σ_3 studied here, from 0 to 1.6 Mbar. In the turnaround region and in the upper branch instabilities and discontinuous changes in structure occur. If an experimental sequence of anisotropic stresses with $|\sigma_1| < |\sigma_3|$ (which could occur experimentally) crosses this region, anomalous changes in structure are indicated. We have not at this point explored instabilities that break the tetragonal symmetry, which would complicate the behavior.

The two-index coefficients c_{ij}, which are symmetric in i and j by definition, must be some average over the four-index elastic constants $B_{ijk\ell}$ and $A_{ijk\ell}$ in [1] and [2]. The existence of the c_{ij} seems clearly justified by the fact that $\delta E + \delta W$ is a function of the $\{\epsilon_i\}$ at a particular set of applied stresses, and the minimum theorem for $\delta E + \delta W$ at equilibrium leads to their elastic and stability properties. The differential quantity $\delta E + \delta W$ is functioning like a δG, although an equilibrium G which is a function of state does not exist. The desired properties

11

of elastic response and stability for crystals in equilibrium under anisotropic stress are deduced from $\delta E + \delta W$ and involve multiple-valued functions a, c, c_{ij} of σ_1 and σ_3.

References

[1] Barron T H K and Klein M L 1965 *Proc. Phys. Soc.* **85** 523
[2] Wallace D C 1972 *Properties of Crystals* (New York: Wiley)
[3] Nye J R 1958 *Physical Properties of Crystals* (Oxford: Clarendon)
[4] Wang J, Li J, Yip S, Phillpot S and Wolf D 1995 *Phys. Rev.* B **52** 12627
[5] Marcus P M, Jona F and Qiu S L 2002 *Phys. Rev.* B **66** 064111
[6] Blaha P, Schwarz K, Madsen G K H, Kvasnicka D and Luitz J 2001 *WIEN2k An Augmented Plane Wave + Local Orbitals Program for Calculating Crystal Properties* (Kalheinz Schwarz, Techn. Universität Wien, Austria), ISBN 3-9501031-1-2
[7] Hohenberg P and Kohn W 1964 *Phys. Rev.* B **136** 864
    Kohn W and Sham L J 1965 *Phys. Rev.* B **140** A1133
[8] Cottenier S 2002 *Density Functional Theory and the Family of (L)APW-Methods: A Step-by-Step Introduction* (Leuven: Instituut voor Kern-en Stralingsfysica) ISBN 90-807215-1-4 (to be found at http://www.wien2k.at/reg_user/textbooks)
[9] Pearson W B 1967 *A Handbook of Lattice Spacings and Structures of Metals and Alloys* vol 2 (Oxford: Pergamon)
[10] Jona F and Marcus P M 2006 *J. Phys.: Condens. Matter* **18** 10881
[11] Akahama *et al* 2006 *Phys. Rev. Lett.* **96** 045505